

# On-demand texture dialling of VO<sub>2</sub> M/B-phase nano-structured films using scanning focused laser irradiation

Lin Hong Yi, Fong Kei Sen, Aznikah Bte Abdul Nizar

Anderson Junior College

Singapore

Dr Zheng Min Rui, Prof Sow Chornng Haur

National University of Singapore

Singapore

## 1.0 BACKGROUND AND PURPOSE OF RESEARCH

Transition metal oxides provide the ultimate spectrum of 3-dimensional crystallographic spatial arrangement with their various polymorphic structures. Vanadium dioxide (VO<sub>2</sub>) exhibits a diversity of polymorphic forms, such as VO<sub>2</sub> (M), VO<sub>2</sub> (R), VO<sub>2</sub> (A), VO<sub>2</sub> (B), and VO<sub>2</sub> (C),<sup>1</sup> offering an unprecedented prospect of paving the way for next generation functional materials with its superior properties, coupled with the possibility of metal-semiconductor,<sup>2</sup> metal-insulator<sup>3</sup> and semiconductor-insulator transitions. VO<sub>2</sub> (B) in particular has piqued the interest of many researchers recently as a promising cathode material for lithium-ion batteries due to its large capacity for Li<sup>+</sup> intercalation.<sup>4</sup> Nevertheless, one major drawback of VO<sub>2</sub> (B) based cathode is its low electronic conductivity.<sup>5</sup> VO<sub>2</sub> (M), on the other hand, has comparatively lower resistance.<sup>6</sup> Therefore, creating a VO<sub>2</sub> (B) and VO<sub>2</sub> (M) hybrid offers the possibility of retaining the Li<sup>+</sup> ion intercalation capacity for VO<sub>2</sub> (B), while at the same time significantly improving the conductivity of the composite material system.<sup>7</sup> Herein, we report a method for on-demand texture dialling of VO<sub>2</sub> (B) nano-structured films grown on strontium titanate substrates to VO<sub>2</sub> (M) using scanning focused laser irradiation. This approach is compatible with the standard production process in the lithium-ion battery industry, and provides complete autonomy and absolute precision. This research catalyses the development of practical devices with VO<sub>2</sub> (B) and opens up new avenues for fundamental research.

## 2.0 HYPOTHESIS

In recent studies, VO<sub>2</sub> (B) has shown to be a promising candidate cathode material for use in lithium ion battery, but with limitations in electronic conductivity. In light of this, we studied the effect of scanning focused laser irradiation

using a 532 nm green laser on VO<sub>2</sub> (B) thin film. We aim to locally induce VO<sub>2</sub> (B) to undergo phase conversion to VO<sub>2</sub> (M) upon focused laser irradiation treatment and by doing so on the surface, provide a VO<sub>2</sub> (B) and VO<sub>2</sub> (M) hybrid that has significantly increased electronic conductivity.

## 3.0 MATERIALS AND METHODS

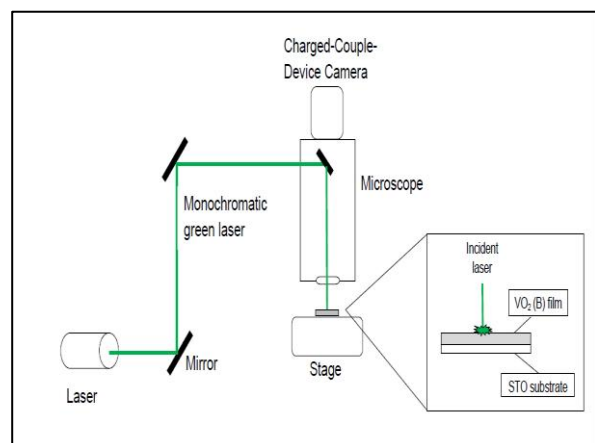


Figure 1. Schematic design of the home-built scanning focused laser irradiation setup with an x-y motorised stage

### Experiment 1 – Laser scanning of 2 rows by 4 columns of squares on VO<sub>2</sub> (B) film

In this experiment, a 532 nm green laser is used to raster squares with dimensions 20 μm x 20 μm on the VO<sub>2</sub> (B) film under room conditions. The stage can be both manually or computer controlled to slide the sample in xy directions to allow the stationary laser to cut patterns on it. In order to investigate how the surface of the VO<sub>2</sub> (B) reacts to laser irradiation, the laser speed used is chosen to fix at 50 μm/s for the top row of squares and 100 μm/s for the bottom row of squares. The laser power is also varied from 25 mW to 55 mW, with a step increment of 10 mW from the first column. (i.e. squares at first column are rastered with 25 mW of

laser power and squares at the 2nd column are rastered with 35 mW of laser power, etc.)

In order to create patterns, the minimum rastering power required to induce a visible modification on the VO<sub>2</sub> (B) surface was tested by a step increment of laser power of 5 mW each time from 0 mW. When the first observable scratch was observed, the power of the laser was immediately measured and recorded by a laser power meter measuring at 532 nm wavelength. After repeated testing conducted at multiple spots on the sample surface, it was discovered that for the faintest scratch to be visible by the human eye, a laser power of  $(17.74 \pm 4.08)$  mW is needed.

After collecting our results, we began to laser scan a 20  $\mu\text{m}$  x 20  $\mu\text{m}$  square in a vertical zigzag manner, starting from a laser power of 25 mW with a computer-controlled raster speed of 50  $\mu\text{m}/\text{s}$  on the top row and 100  $\mu\text{m}/\text{s}$  on the bottom row. With the raster speed of each row respectively kept constant, the power is increased by 10 mW between each rastered area from left to right, and the process is repeated for both rows, until we obtain 2 rows by 4 columns of squares, with the 2 squares on the 4th column scanned by a power of 55 mW under the respective speed of the laser scanning. (See figure 2 for illustration)

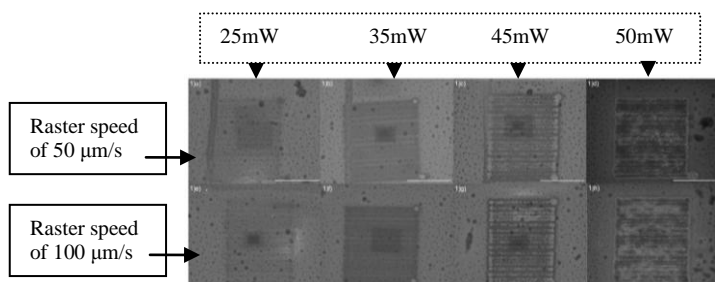


Figure 2. SEM images of each individual square using a JOEL 6700F field-emission SEM. Raster speed for all squares at the top row and bottom row are 50  $\mu\text{m}/\text{s}$  and 100  $\mu\text{m}/\text{s}$  respectively. There is a step increment of the laser power of 10 mW from left to right. (Diagram is for scale: The scale bar at the bottom right corner of each picture represents 10  $\mu\text{m}$ ).

#### Experiment 2 - Large area scan sample

To prepare a large-area scan sample for global measurements such as PPMS (Physical Property Measuring System), XRD (X-Ray Diffraction) and XPS (X-ray Photoelectron Spectroscopy), we rastered the sample with a laser power of 55 mW and a raster speed of 100  $\mu\text{m}/\text{s}$  uniformly in a zigzag manner such that we would receive the optimal sample surface where VO<sub>2</sub> (B) has speculatively undergone a phase change to the M-phase.

#### Experiment 3 – Raman spectroscopy

In this experiment, we used a Renishaw inVia Raman microscope with 532 nm green excitation laser with very low intensity to illuminate the surface of the rastered VO<sub>2</sub> (B) sample in a backscattering geometry. The Raman-scattered light component from the laser after it comes in contact with the sample is measured against the Raman shift. Results were then collected and compared with different rastered sample and substrates.

#### Experiment 4 – Temperature-dependent resistivity measurement using a Physical Property Measurement System (PPMS)

This experiment is carried out using a Quantum Design PPMS to investigate the I-V relationship of the rastered VO<sub>2</sub> (M) sample under a varied temperature in order to deduce if its electrical conductivity has been affected by the laser treatment. The sample is lowered into the PPMS and the sample is exposed to a temperature ranging from 300 K – 400 K in a vacuum condition. The I-V relationship is recorded down using computer software connected to the PPMS.

## 4.0 RESULTS AND DISCUSSION

### Results 1 – Scanning Electron Microscope (SEM) images of laser scanning of 2 rows by 4 columns of squares on VO<sub>2</sub> (B) film

From the results obtained from experiment 1, as the laser power increases by 10 mW each time across the row, the rastered traces become rougher and darker. However, as the laser scanning speed increases down the column, the surface texture of the sample seemed similar (seen in figure 2). Thus, we deduce that the out of the 2 physical properties we varied of the laser, power changes impact the rastered surface more evidently. Also, when the laser power is increased to 55 mW, needle-shaped microcrystals can be seen forming on the surface (seen in figure 3). We suspected that a phase change to the M-phase has occurred on the VO<sub>2</sub> (B) sample.

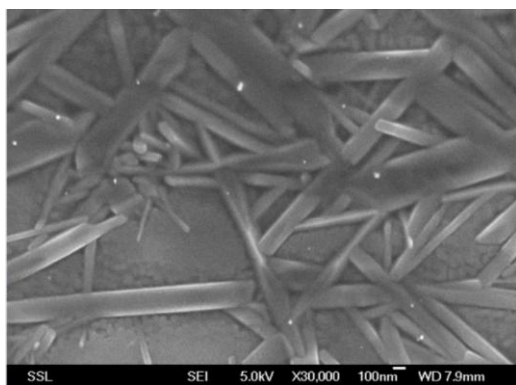


Figure 3. Zoomed in SEM image of the crystals formed on the square at Figure 1(d) above.

### Results 2 – Large area scan sample

Moving on, we prepared a large-area scanned sample (3 mm x 3 mm) for characterization tests to unfold some potential changes in physical properties that might arise due to laser treatment as mentioned earlier (as seen in figure 4).

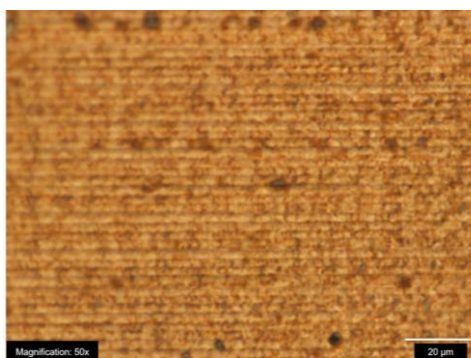


Figure 4. OM image of the large area scan sample at bright field mode.

### Results 3 – Raman spectroscopy

The first characterisation test we carried out was the Raman spectroscopy test.

There were no changes in the shift where peaks occurred as compared to the substrate signal, which shows that VO<sub>2</sub> (B) phase has metallic properties. However, the intensity of the shift did reduce when the rastered sample was used, indicating that the sample is either relatively thick or has a higher absorption coefficient at 532 nm, and does not easily allow the laser light to pass through. The bright rastered graph, in which crystallisation occurred, has lower intensity compared to the rastered graphs, in which crystallisation did not occur, indicating further that the crystals reflect the light more and allow less light to pass through and further confirming that the sample was crystallised and it possessed metallic properties.

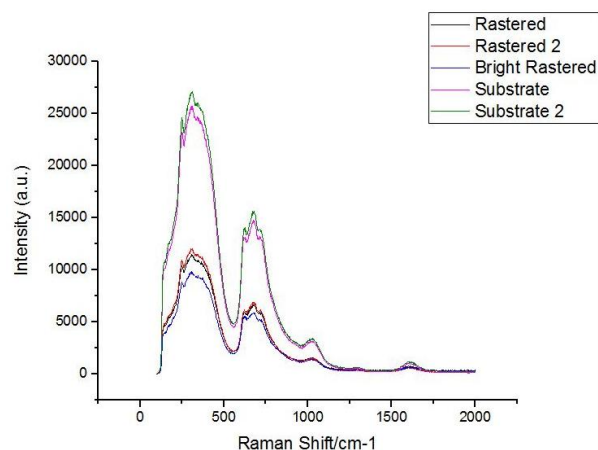


Figure 5. Relationship of intensity against Raman shift of the sample (actual).

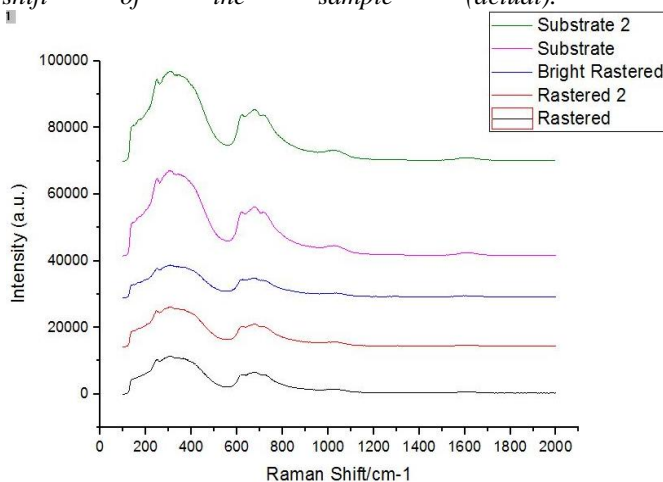


Figure 6. Relationship of intensity against Raman shift of the sample (stacked).

### Results 4 - PPMS

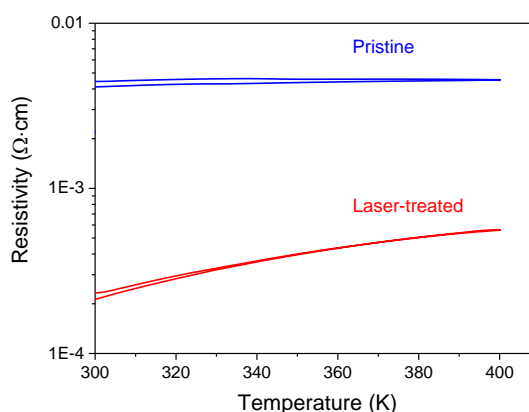


Figure 7. Temperature-dependent resistivity plots for pristine VO<sub>2</sub> (B) film on STO substrates, and after large-area laser treatment.

From the results we gathered from the PPMS test, it was discovered that the resistivity of the laser treated sample decreased by approximately fifteen times compared to the pristine sample at every temperature level. Henceforth it is deduced that the laser treated sample with lower resistivity possessed greater metallic properties and a potential hybrid of VO<sub>2</sub> (M) and VO<sub>2</sub> (B) that has been created allows much better electrical conduction.

## 5.0 CONCLUSION RECOMMENDED USE FOR FUTURE WORK

In conclusion, VO<sub>2</sub> (B) that has been laser treated by the green 532 nm laser allows for selective growth of VO<sub>2</sub> (M) on our sample. Through systematic analysis of the physical property measurement system graphs of the modified and unmodified VO<sub>2</sub> (B) thin film, we have discovered that VO<sub>2</sub> (M) can indeed co-exist with VO<sub>2</sub> (B) in a controlled manner, and this hybrid has significantly increased electron conductivity of fifteen folds. In terms of application, we discover that if VO<sub>2</sub> (B) films were to be produced for use as cathode material for lithium-ion battery, it could be significantly improved by undergoing quick laser treatment which would improve the performance of these lithium-ion batteries. This strategy offers a facile and robust alternative to modify VO<sub>2</sub> (B) for use as cathode material in lithium-ion batteries.

Future works for this experiment could be using different surface areas of laser rastering to determine the optimum area in which desirable electron conductivity is achieved. This strategy offers a facile and robust alternative to modify VO<sub>2</sub> (B) material for further research by using different patterns of laser rastering to modify the VO<sub>2</sub> (B) sample so as to provide an efficient pathway for electrons to conduct.

## 6.0 REFERENCES

<sup>1</sup>Amar Srivastava, Helene Rotella, Surajit Saha, Banabir Pal, Gopinadhan Kalon, Sinu Mathew,

Mallikarjuna Motapothula, Michal Dykas, Ping Yang, Eiji Okunishi, D. D. Sarma, and T. Venkatesan, *Selective growth of single phase VO<sub>2</sub>(A, B, and M) polymorph thin films*, *APL Materials* **3**, 026101 (2015)

<sup>2</sup>Armando Rúa, Ramón D. Díaz, Sergiy Lysenko, and Félix E. Fernández, *Semiconductor-insulator transition in VO<sub>2</sub> (B) thin films grown by pulsed laser deposition*, *Journal of Applied Physics* **118**, 125308, (2015)

<sup>3</sup>Serena A. Corr, Madeleine Grossman, Yifeng Shi, Kevin R. Heier, Galen D. Stucky and Ram Seshadriab, *VO<sub>2</sub>(B) nanorods: solvothermal preparation, electrical properties, and conversion to rutile VO<sub>2</sub> and V<sub>2</sub>O<sub>3</sub>*, *Journal of Materials Chemistry* **19**, 4362 – 4367 (2009)

<sup>4</sup>Shubin Yang, Yongji Gong, Zheng Liu, Liang Zhan, Daniel P. Hashim, Lulu Ma, Robert Vajtai, and Pulickel M. Ajayan, *Bottom-up Approach toward Single-Crystalline VO<sub>2</sub> Graphene Ribbons as Cathodes for Ultrafast Lithium Storage*, *Nano Letters* **13**, 1596 – 1601 (2013)

<sup>5</sup>Rui, Xianhong, *Nanostructured vanadium-based cathodes for rechargeable lithium ion batteries* Doctoral Thesis, School of Materials Science and Engineering, Nanyang Technological University (2014)

<sup>6</sup>Karel J1, ViolBarbosa CE, Kiss J, Jeong J, Aetukuri N, Samant MG, Kozina X, Ikenaga E, Fecher GH, Felser C, Parkin SS, *Distinct electronic structure of the electrolyte gate-induced conducting phase in vanadium dioxide revealed by high-energy photoelectron spectroscopy*, *ACS Nano* **8**, 5784 – 5789 (2014)

<sup>7</sup>Aiping Chen, Zhenxing Bi, Wenrui Zhang, Jie Jian, X. Jia, Haiyan Wang, *Textured metastable VO<sub>2</sub>(B) thin films on SrTiO<sub>3</sub> substrates with significantly enhanced conductivity*, *Applied Physics Letters* **104**, 071909, (2014)